JOURNAL OF AGRICULTURAL AND FOOD CHEMISTRY

Article

pubs.acs.org/JAFC

In Vitro Suppression of Growth of Murine WEHI-3 Leukemia Cells and in Vivo Promotion of Phagocytosis in a Leukemia Mice Model by Indole-3-carbinol

Hsu-Feng Lu,[†,‡] Wei-Lin Tung,[§] Jai-Sing Yang,[⊥] Fang-Ming Huang,[∥] Ching-Sung Lee,[‡] Yi-Ping Huang,[#] Wen-Yen Liao,[$] Yung-Liang Chen,*[,▽] and Jing-Gung Chung*[,¶,□]

[†]Department of Clinical Pathology, Cheng Hsin General Hospital, Taipei 112, Taiwan

[‡]College of Human Ecology, Fu-Jen Catholic University, New Taipei 242, Taiwan

[§]School of Pharmacy, China Medical University, Taichung 404, Taiwan

[⊥]Department of Pharmacology, China Medical University, Taichung 404, Taiwan

[∥]Department of Surgical Intensive Care Unit, Far Eastern Memorial Hospital, New Taipei 220, Taiwan

[#]Department of Physiology, China Medical University, Taichung 404, Taiwan

[$]School of Traditional Chinese Medicine, Chang Gung University, Taoyuan 333, Taiwan

[▽]Department of Medical Laboratory Science and Biotechnology, Yuanpei University, Hsinchu 300, Taiwan

[¶]Department of Biological Science and Technology, China Medical University, Taichung 404, Taiwan

[□]Department of Biotechnology, Asia University, Taichung 413, Taiwan

ABSTRACT: Indole-3-carbinol (I3C), a potential anticancer substance, can be found in cruciferous (cabbage family) vegetables, mainly cauliflower and Chinese cabbage. However, the bioactivity of I3C on the apoptotic effects of murine leukemia WEHI-3 cells and promotion of immune responses in leukemia mice model are unclear. In this study, we investigated the effect of I3C on cell-cycle arrest and apoptosis in vitro and immunomodulation in vivo. I3C decreased the viable WEHI-3 cells and caused morphological changes in a concentration- and time-dependent manner. I3C also led to G0/G1 phase arrest, decreased the levels of cyclin A, cyclin D, and CDK2, and increased the level of $p21^{WAF1/CIP1}$. Flow cytometric analyses further proved that I3C promoted ROS and intracellular Ca^{2+} production and decreased the levels of $\Delta\Psi_m$ in WEHI-3 cells. Cells after exposure to I3C for 24 h showed DNA fragmentation and chromatin condensation. Comet assay also indicated that I3C induced DNA damage in examined cells. I3C increased the levels of cytochrome c, FADD, GADD153, GRP78, and caspase-12 as well as induced activities of caspase-3, -8, and -9. Moreover, I3C attenuated NF-κB DNA binding activity in I3C-treated WEHI-3 cells as shown by EMSA and Western blotting analyses. In the in vivo study, we examined the effects of I3C on WEHI-3 leukemia mice. Results showed that I3C increased the level of T cells and decreased the level of macrophages. I3C also reduced the weights of liver and spleen, and it promoted phagocytosis by macrophages as compared to the nontreated leukemia mice group. On the basis of our results, I3C affects murine leukemia WEHI-3 cells both in vitro and in vivo.

KEYWORDS: *indole-3-carbinol, apoptosis, WEHI-3 leukemia cells, leukemia model, phagocytosis*

INTRODUCTION

Natural chemopreventives are gaining interest for cancer prevention. For example, indole-3-carbinol, isoflavones, curcumin, apigenin, and (−)-epigallocatechin-3-gallate (EGCG) inhibit the carcinogenic process and thus reduce the risk of many types of cancer.[1] Programmed cell death type I (apoptosis) is characterized by morphological changes, including cell shrinkage, chromatin condensation, and internucleosomal cleavage of genomic DNA. Three major apoptotic pathways have been characterized: the death receptor-regulated pathway (or extrinsic signaling), mitochondria-mediated apoptosis pathway (intrinsic pathway), and the endoplasmic reticulum (ER) stress-mediated apoptosis pathway.[2] The death receptor-mediated pathway is started by interaction of the ligand with its death receptor and then sequentially recruits receptor-associated death domains, caspase-8 and caspase-3.[3] The mitochondria-mediated pathway involves the alteration of mitochondrial membrane permeability, thereby promoting the release of cytochrome c, apoptosis protease-activating factor-1 (Apaf-1), and procaspase-9 from mitochondria, activates caspase-9, and then later activates caspase-3.[3] Many reports suggest that caspase-12 and disruption of calcium (Ca^{2+}) homeostasis are important for the ER stress-mediated pathway.[4,5] The ER serves as the major reservoir for free Ca^{2+}, and Ca^{2+} transport from the ER to the mitochondria is required for the initiation of programmed cell death by apoptotic inducers.[5]

Control of cell cycle and apoptosis presents a major target for preventive and therapeutic intervention in cancers. Central targets of cell cycle regulation pathways are cyclin/cyclin-dependent

Received: December 8, 2011
Revised: July 7, 2012
Accepted: July 9, 2012
Published: July 9, 2012

kinase (CDK) protein complexes. The activation of cyclin/CDK complexes drives cells from the G1 phase into the S phase of the cell cycle. The complexes of cyclin D/CDK4 and cyclin D/CDK6 as well as cyclin A/CDK2 and cyclin E/CDK2 are especially important in the transition from G1 to S phase.[6,7] CDK inhibitors (CKIs) such as $p21^{waf1/cip1}$ are known to bind to the cyclin/CDK complexes of CDK2, CDK4, and CDK6 following DNA damage to inhibit cyclin/CDK complex catalytic activity and induce cell-cycle arrest and apoptosis.[8]

Indole-3-carbinol (I3C) is a natural product isolated from cruciferous species. In vivo studies have demonstrated that I3C inhibited hepatocarcinogenesis, skin carcinogenesis, and colon cancer in animal experiments.[9,10] Also, I3C inhibited the growth of MDA-MB-231 human breast cancer cells, LNCaP prostate cancer cells, and HT-29 colon cancer cells.[11−13] I3C promoted G0/G1 phase arrest and induced apoptotic effects in human cancer cells, including human breast cancer, melanoma, and prostate cancer.[14−16] Additionally, I3C suppressed nuclear factor-kappaB (NF-κB) and IκBα kinase activation, causing inhibition of expression of NF-κB-regulated antiapoptotic and metastatic gene products and enhancement of apoptosis in myeloid leukemia cells from acute myelogenous leukemia (AML) patients.[17] However, the molecular mechanisms of I3C-inhibited the growth and -induced apoptotic death of murine acute myelomonocytic leukemia WEHI-3 cells have not been fully elucidated. The aim of this study was to emphasize the mechanism of antileukemia action of I3C in murine WEHI-3 leukemia cells in vitro. We also investigated the antileukemic effects of I3C in an animal model of leukemia in vivo.

MATERIALS AND METHODS

Materials and Reagents. Reagents used were as follows: Indole-3-carbinol, 3-(4,5-dimethylthiazol-2-yl)-2,5-diphenyltetrazolium bromide (MTT), RNase A propidium iodide (PI), and anti-β-actin (Sigma-Aldrich Corp., St. Louis, MO); RPMI-1640, fetal bovine serum (FBS), trypsin−EDTA and penicillin−streptomycin (Gibco/Life Technologies, Grand Island, NY); DAPI, H_2DCFDA, Fluo-3/AM, and $DiOC_6$ (Molecular Probes/Life Technologies, Eugene, OR). The antibodies for CDK4, CDK6, GAPDH, Fas/CD95, FADD, cytochrome c, GADD153, GRP78, NF-κB (p50), NF-κB (p65), and PCNA were purchased from Santa Cruz Biotechnology, Inc. (Santa Cruz, CA). Anticyclin A, anticyclin D, and anticaspase-12 were obtained from BD Pharmingen (San Diego, CA). Anticyclin E (cat. 07-687), anti-CDK2 (cat. 05-596), anti-$p21^{WAF1/CIP1}$ (cat. 05-345), and anti-p53 (cat. 04-241) were bought from Merck Millipore (Bedford, MA). Horseradish peroxidase-conjugated antirabbit, antimouse, and antigoat IgG secondary antibodies were purchased from Santa Cruz Biotechnology, Inc.

In Vitro Experiments. *Cell Culture and MTT Assay.* WEHI-3, a murine acute myelomonocytic leukemia cell line, was obtained from the Food Industry Research and Development Institute (Hsinchu, Taiwan). Cells were maintained in RPMI-1640 containing 10% FBS with 100 units/mL penicillin and 100 μg/mL streptomycin. For MTT assay, WEHI-3 cells (2×10^4 cells/100 μL per well) were plated in 96-well plates and exposed to I3C as detailed in respective experiments for 24 and 48 h. Then about 10 μL of MTT (5 mg/mL) was added to each well and incubated for an additional 4 h in the dark at 37 °C. The medium was then aspirated from the wells, and the blue formazon product was dissolved in a 100 μL of DMSO. The plates were read at OD 570 nm using a spectrophotometric plate reader (Bio-Rad, Tokyo, Japan).[18,19] Each data point was replicated in triplicate.

Observation for Morphological Changes and DNA Content Analysis. WEHI-3 cells (2×10^5 cells/well) were placed in 24-well plates and then treated with 0, 50, 100, or 150 μM I3C for 24 and 48 h. After that, cells were visualized and photographed under a phase-contrast microscope before being harvested.[18] The trypsinized cells were washed in PBS and fixed in 70% ethanol at −20 °C overnight. After being washed, the cells were incubated in 0.5% Triton X-100 containing 1 mg/mL of RNase A at 37 °C for 30 min and then stained with PI (40 μg/mL). Fluorescence intensity in the FL-2 channel was monitored via flow cytometry (FACSCalibur, BD Biosciences, Franklin Lakes, NJ) as previously described.[18,19]

4′,6-Diamidino-2-phenylindole (DAPI) Staining. WEHI-3 cells (2×10^5 cells/well) were placed in 24-well plates before being treated with 0, 50, and 150 μM I3C for 24 h. The cells were fixed by 3% (w/v) formaldehyde in PBS for 15 min and washed with PBS, and 0.1% Triton-X 100 was added. After 20 min, cells then were stained with 10 μg/mL DAPI (Molecular Probes/Invitrogen Corp.) for 30 min at 37 °C. The stained cells were observed under a fluorescence photomicroscope (Olympus, Japan) to study the morphological change of cells during the apoptosis process.[20,21]

Comet Assay. Each slide of 5000−10 000 cells was mixed with 150 μL of 0.5% low-melting agarose (Sigma-Aldrich Corp.) and held at 37 °C. The agarose was spread into single layers on ordinary, clear-glass slides that had been pretreated with a small amount of agarose and air-dried. After solidification on a chilled plate, the slides were transferred to the same lysis buffer (2.5 M NaCl, 10 mM Tris-HCl, 0.1 M EDTA, 1% (v/v) Triton X-100, pH 8−10) and held on ice for 1 h, when appropriate in the presence of PI as described above.[20,22] Individual results from the comet assay were quantitated and analyzed by measuring the amounts of comet length (fold of control) of each cell using CometScore software version 1.5 (Tritek Corp., Sumerduck, VA).

DNA Fragmentation by Agarose Gel Electrophoresis. WEHI-3 cells (1×10^6 cells/well) were placed in six-well plates and then treated with 0, 50, 100, and 150 μM I3C for 24 h. Cells were collected and lysed in 0.5 mL of DNA lysis buffer (20 mM Tris-HCl, 10 mM EDTA, and 0.2% Triton X-100). The cell lysate was treated with 0.1 μg/mL proteinase K and stored at 50 °C overnight, and then 50 μg/mL RNase A was added at 37 °C for 30 min. After centrifugation, supernatant was precipitated by 2-propanol. The DNA pellets were rinsed with 70% ethanol and dissolved in TBE buffer (AMRESCO, Solon, OH). Gel electrophoresis used 1.5% agarose gel, and DNA laddering fragmentation was visualized by ethidium bromide (EtBr, Molecular Probes/Life Technologies) staining under UV light.[21]

Determination of Intracellular ROS Production, Mitochondrial Membrane Potential ($\Delta\Psi_m$), and Ca^{2+} Release. ROS generation was measured after staining the cells with H_2DCFDA. Following exposure to 100 μM I3C, the cells were trypsinized and washed with ice-cold PBS. We then added 500 μL of PBS containing 10 μM H_2DCFDA and incubated the cells for 30 min at 37 °C. The fluorescence emission from DCF was analyzed by flow cytometry.[23,24] Changes in the $\Delta\Psi_m$ level were monitored after staining with $DiOC_6$. Cells after exposure to I3C were trypsinized, washed with PBS, and then stained with $DiOC_6$ (1 μM) for 30 min at 37 °C.[25,26] The level of intracellular Ca^{2+} release was measured after staining the cells with Fluo-3/AM and analyzed by flow cytometry.[25] After I3C treatment, the cells were trypsinized, washed in PBS, and then stained with Fluo-3/AM (2.5 μg/mL) for 40 min at 37 °C. The percentage of green fluorescence was estimated by flow cytometry.

Caspases Activity Assay. WEHI-3 cells (1×10^6 cells/well) were placed in six-well plates and exposed to 100 μM I3C for 3, 6, 12, and 18 h. Cells were collected in lysis buffer (50 mM Tris-HCl, 1 mM EDTA, 10 mM EGTA, 10 mM digitonin, and 2 mM DTT) on ice for 10 min. The lysates were centrifuged at 15 000*g* at 4 °C for 10 min. Cell lysates (50 μg protein) were incubated with caspase-3, -9, and -8 specific substrates (Ac-DEVD-pNA, Ac-LEHD-pNA, and Ac-IETD-pNA; R&D Systems, Minneapolis, MN) with reaction buffer in a 96-well plate at 37 °C for 1 h. The caspase activity was determined by measuring OD 405 nm of the released pNA as described elsewhere.[21]

Western Blotting Analysis. Total cell lysates or nuclei fractions were prepared as previously described.[25,26] The protein contents consisted of total cell lysate fractions using the BCA protein assay kit (Pierce Biotechnology, Inc., Rockford, IL). The proteins were separated on sodium dodecyl sulfate polyacrylamide gel electrophoresis (SDS-PAGE) and transferred onto the Immobilon-P transfer membrane PVDF (Cat. IPVH00010, Merck Millipore). The blots were blocked in nonfat dry milk in PBST (20 mM Tris-HCl, pH 7.5, 150 mM NaCl, and 0.1% Tween 20) and incubated with specific primary

antibodies. The blots were then incubated with antimouse, antirabbit, or antigoat horseradish peroxidase-conjugated secondary antibodies. Signals were detected by means of an enhanced chemiluminescence (ECL) method using Immobilon Western Chemiluminescent HRP substrate (cat. WBKLS0500, Merck Millipore). The relative abundance of each band was quantified using NIH ImageJ (version 1.43) for Windows.[27]

Confocal Laser Microscopy Assay. The localization of cytochrome c was examined by confocal laser microscopy assay indirectly. WEHI-3 cells (5×10^4 cells) were maintained on four-well chamber slides and treated with 100 μM I3C for 24 h. Cells were then fixed with 3% formaldehyde in PBS for 15 min and permeabilized with 0.1% Triton-X 100 for 1 h with blocking of nonspecific binding sites using 2% BSA. The cytochrome c antibody (1:100 dilution; Santa Cruz Biotechnology, Inc.) was applied for overnight and then followed by 1 h of incubation with FITC-conjugated goat antirabbit IgG at 1:100 dilutions (Santa Cruz Biotechnology, Inc.). Mitochondria were counterstained with MitoTracker Red CMXRos (Molecular Probes/Life Technologies). Photomicrographs were obtained as previously described.[28]

Electrophoretic Mobility Shift Assay (EMSA). WEHI-3 cells were seeded at 5×10^6 cells per 100-mm dish and incubated with or without 100 μM I3C for 6 and 12 h. At the end of incubation, nuclear extracts were obtained using a Nuclear Extraction Kit (Panomics Inc., Redwood, CA) according to the instructions provided by the manufacturer and quickly frozen at −70 °C for further determinations. NF-κB binding to DNA was determined by using an EMSA Gel Shift Kit (Panomics Inc.) according to the manufacturer's protocol and experimental procedures. The sequence for the NF-κB motif-containing biotin-labeled probe is 5′-GGGGAATCTCCCGGGGACTTTCC-3′. Nuclear protein (2.5 μg) from each sample was used to detect the DNA binding activity of NF-κB using a commercially available EMSA kit with a biotin-labeled NF-κB consensus probe essentially based on the instructions of the manufacturer (Panomics Inc.). Each sample was separated on 6.0% nondenaturing polyacrylamide gel, and shifted bands that corresponded to protein/DNA complexes were captured by an HRP-based detection system. Signals were incubated with the substrate of the ECL kit (Merck Millipore) and detected by chemiluminescent imaging. Experiments were performed in excess of three times.[29]

In Vivo Experiments. *I3C Treatment.* Fifty BALB/c mice at the age of 8 weeks and about 22−28 g in weight were obtained from the Laboratory Animal Center, College of Medicine, National Taiwan University (Taipei, Taiwan). All animals then were divided into 5 groups. Each group contains 10 animals. Group I was control; group II was treated with olive oil (vehicle). Group III was intraperitoneally injected with WEHI-3 (1×10^5 cells/mouse) only for 2 weeks. Group IV and V were intraperitoneally injected with WEHI-3 (1×10^5 cells/mouse) for 2 weeks and then orally treated with I3C (60 and 120 mg/kg body weight) in olive oil. All animals were given the above doses daily for up to 2 weeks by oral gavage before being weighed. Our in vivo experiment has been approved by the Institutional Animal Care and Use Committee (IACUC) of China Medical University (no. 101-05-B).

Blood Samples and Immunofluorescence Staining. At the end of the above experiments, about 1 mL of blood was collected from each animal of each group and was treated with 1× Pharm Lyse lysing buffer (BD Biosciences, San Jose, CA) for lysing of the red blood cells, followed by centrifugation for 5 min at 1500 rpm at 4 °C. The isolated white blood cells were examined for cell markers, including CD3, CD19, CD11b, and Mac-3 based on the staining with anti-CD3-FITC, -CD19-PE, -CD11b-FITC, and -Mac-3-PE antibodies (BD PharMingen, San Diego, CA). Cells were determined for the cell marker levels by flow cytometry as described elsewhere.[26,30]

Spleen and Liver Samples. Animals from each group were weighed before blood was sampled. The isolated individual liver and spleen samples were weighed individually.[26,30]

Assay for Phagocytosis by Macrophages. At the end of the above treatments, macrophages were isolated from peripheral blood mononuclear cells (PBMC) and peritoneum of each mouse (control and experiment groups). Isolated cells were placed in FACS tubes, and 50 μL of *E. coli*−FITC was added according to PHAGOTEST kit manufacturer's instructions (Glycotope Biotechnology GmbH, Heidelberg, Germany). All cells from each treatment were shaken in a shaker bath for 30 min at 37 °C, the supernatant was discarded, and the pellets were subjected to DNA staining for determining phagocytic activity as described previously.[19] Each sample was analyzed by flow cytometery and CellQuest software (BD Biosciences).

Statistical Analyses. Data are expressed as mean ± SD of the values from the number of experiments. The values were analyzed by Student's *t* test or one-way ANOVA followed by Dunnett's test. The level of significance was set at $p < 0.05$ in all cases.

RESULTS

In Vitro Studies. *Antiproliferative Effects of I3C in WEHI-3 Cell Line.* The WEHI-3 cells were treated with I3C at concentrations of 25, 50, 75 100, and 150 μM for various time periods. Cell viability was counted by MTT assay for 24 and 48 h. As shown in Figure 1A, I3C exhibited a concentration- and time-dependent antiproliferative action in WEHI-3 cells The concentration required to inhibit growth by 50% (IC_{50}) for WEHI-3 was approximately 100 μM. As presented in Figure 1B,

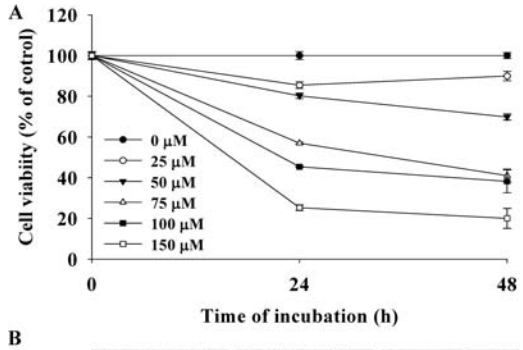

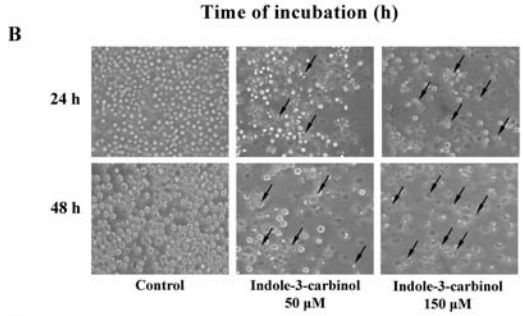

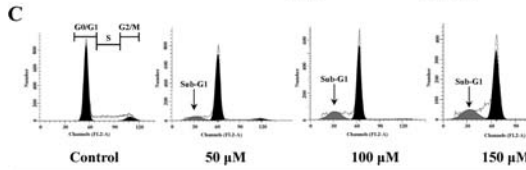

Concentration	Control	50 μM	100 μM	150 μM
Sub-G1 phase (%)	0.11±0.02	14.14±2.28	19.88±2.54	23.38±2.59
G0/G1 phase (%)	63.33±1.00	89.33±1.27*	93.72±0.49*	95.40±1.24*
S phase (%)	29.87±0.68	6.92±0.52	4.42±0.91	3.63±1.14
G2/M phase (%)	6.08±0.66	3.76±0.75	1.86±0.66	0.98±0.68

Figure 1. I3C affected the percentage of viable cells, morphological changes, and cell cycle distribution in WEHI-3 leukemia cells. Cells were exposed to various concentrations of I3C for 24 or 48 h. The percentage of viable cells was measured by MTT assay (A), and morphological changes were observed using a phase-contrast microscope (B) for WEHI-3 leukemia cells in response to I3C. The black arrow (↑) displays the shrinkage and rounding of apoptotic cells. For cell cycle progression analysis (C), WEHI-3 cells were treated with 50, 100, and 150 μM I3C for 24 h followed by incubation with PI solution, and DNA content was immediately analyzed by flow cytometry as described in Materials and Methods. The results are indicated as mean ± SD of three experiments. *$p < 0.05$, significantly different compared with untreated control. Each experiment was repeated three times with similar results.

the morphological changes of WEHI-3 cells were promoted with increasing concentrations of I3C. Apparently I3C led to cytotoxic effects based on the decreased number of cells and the increased cellular debris. To investigate the mechanisms of I3C-induced cytotoxic responses in WEHI-3 cells, cells were treated with I3C at concentrations of 50, 100, and 150 μM for 24 h and then analyzed for DNA content by flow cytometry. As shown in Figure 1C, I3C induced rest and increased the sub-G1 nuclei population in WEHI-3 cells in a concentration-dependent accumulation.

Selective Effects of I3C on Protein Expression of G0/G1-Acting Cell Cycle Components. To reveal the mechanisms of I3C-induced G0/G1 arrest, we investigated the protein expression of G1-acting cyclin (cyclin A, cyclin D, and cyclin E), CDKs (CDK2, CDK4, and CDK6), and CDKI ($p21^{WAF1/CIP1}$) in I3C-treated WEHI-3 cells. As shown in Figure 2, in the three

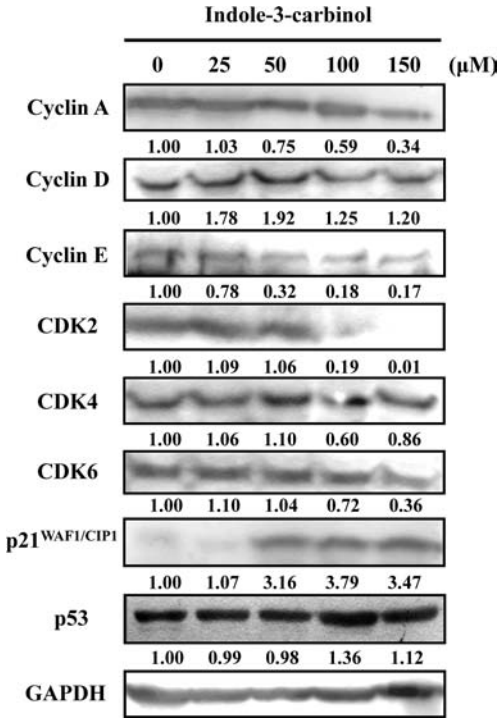

Figure 2. Change in I3C-induced G1-acting protein levels in WEHI-3 cells as shown by Western blotting analysis. Cells were treated with I3C at 25, 50, 100, and 150 μM concentrations for 24 h. Total protein extracts were analyzed by immunoblotting with antibodies specific to cyclin A, cyclin D, cyclin E, CDK2, CDK4, CDK6, and $p21^{WAF1/CIP1}$. Similar results were obtained from three independent experiments.

G1-acting CDKs (CDK2, CDK4, and CDK6), only CDK2 protein levels were strongly down-regulated in response to I3C treatment. I3C also decreases the proteins level of cyclin A and cyclin E and stimulated the protein production of the $p21^{WAF1/CIP1}$and p53. Our results suggest that I3C-mediated cell-cycle arrest of WEHI-3 cells was related to cyclin/CDK activity and $p21^{WAF1/CIP1}$ and p53 protein levels.

Induction of Apoptosis, DNA Damage, and DNA Fragmentation by I3C. To further verify whether cell death caused by I3C was induced through DNA damage and apoptosis in WEHI-3 cells, we assessed the nuclear morphological changes by DAPI staining, and DNA breaks by single cell gel electrophoresis/comet assay. As shown in Figure 3A, after 24-h incubation with 50 and 150 μM I3C, the cells exhibited nuclear shrinkage and chromatin condensation. Less than 1% of the control cells

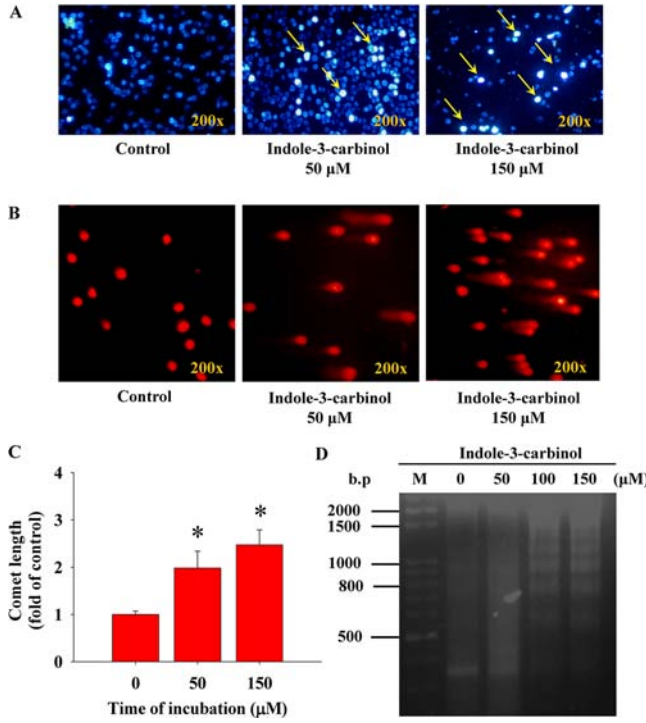

Figure 3. Induction of DNA damage and apoptosis by I3C in WEHI-3 cells. (A) Nuclear morphology of WEHI-3 cells was determined with DAPI staining (at a 200× magnification) after a 24-h treatment with I3C and use of a fluorescence photomicroscope. The arrow (↑) means chromatin condensation (an apoptotic characteristic). (B) DNA breaks by single cell gel electrophoresis/comet assay of WEHI-3 cells after 24 h of treatment with I3C. (C) Results from the comet assay were quantitated using CometScore software. (D) I3C effects of DNA damage in WEHI-3 cells as shown by gel electrophoresis. WEHI-3 cells were incubated with I3C at various concentrations for 24 h, and then the DNA degradation was analyzed with gel electrophoresis, as described in Materials and Methods. The representative data are presented from three separate experiments, and each bar represents the mean ± SD calculated from three independent experiments.

showed evidence of DNA damage in the form of the typical tail formation (Figure 3B,C). WEHI-3 cells after exposure to I3C exhibited a concentration-dependent increase in DNA damage. As shown in Figure 3D from DNA agarose gel electrophoresis, DNA extracted from I3C-treated WEHI-3 cells was fragmented into a laddering pattern. Our results indicate that I3C induced apoptotic cell death and DNA damage in WEHI-3 cells.

Induction of Intracellular ROS Level, $\Delta\Psi_m$ Change, and the Production of Intracellular Ca^{2+} by I3C. To examine whether the mitochondria and/or ER signaling pathway is involved in I3C-induced cell death, the intracellular ROS level, the $\Delta\Psi_m$ changes, and the intracellular production of Ca^{2+} were measured. As shown in Figure 4, I3C significantly decreased the level of $\Delta\Psi_m$ (Figure 4B) and increased the levels of ROS (Figure 4A) and intracellular Ca^{2+} production (Figure 4C) when the cells were treated for 0.5, 1, 5, and 10 h. Our results suggest that activation of the mitochondrial dysfunction and Ca^{2+} signaling pathway may be involved in I3C-induced apoptosis and that ROS plays an important role in WEHI-3 cells during apoptosis.

I3C-Induced Apoptosis Is Mediated by the Activations of Caspase-8, Caspase-9, and Caspase-3. Caspase activation plays a key role in the induction of apoptosis. We investigated the I3C-treated WEHI-3 cells for caspase-9, caspase-8, and

dx.doi.org/10.1021/jf300963t | J. Agric. Food Chem. 2012, 60, 7634−7643

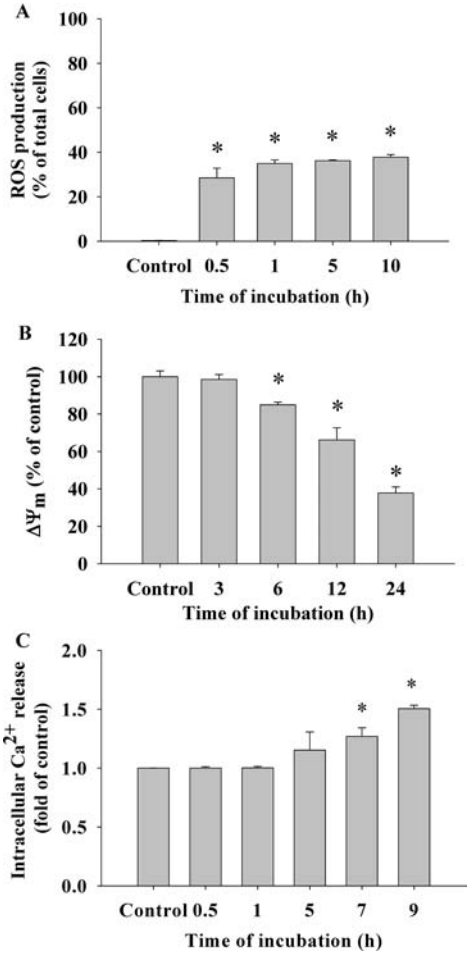

Figure 4. Flow cytometric analyses of ROS production (A), loss of $\Delta\Psi_m$, (B) and Ca^{2+} production (C) in WEHI-3 cells treated with I3C for various periods of time. The WEHI-3 cells were exposed to 100 μM I3C to detect the changes in ROS production, loss of $\Delta\Psi_m$, and intracellular Ca^{2+} release. The 0 h time point was defined as control. Results are expressed as the percentage of cells that were stained by H_2DCFDA, $DiOC_6$, and Fluo-3/AM specific dyes, determined by flow cytometry as described in Materials and Methods. The values represent the mean ± SD of three independent experiments. *p < 0.05, differs significantly between I3C treatment and control sample.

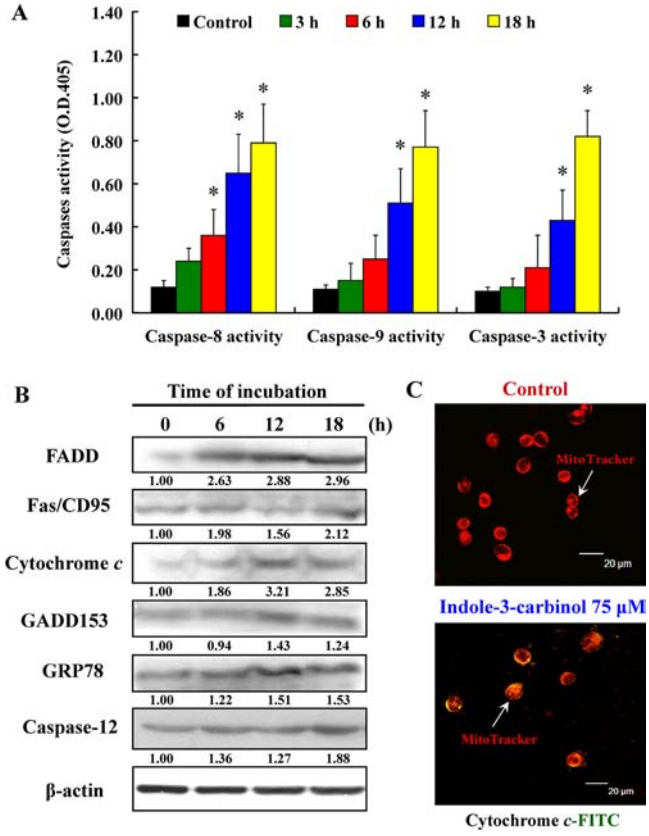

Figure 5. (A) Effects of I3C-induced caspase activity and apoptosis. (B) I3C-triggered apoptosis reflected in protein levels of WEHI-3 cells determined by Western blotting analysis. (C) I3C-promoted release of cytochrome c from mitochondria determined by confocal laser microscopy. The arrow (↑) shows mitochondria after being stained with MitoTracker Red CMXRos in WEHI-3 cells. Scale bar = 20 μm. For caspase activity, cells were stimulated with 100 μM I3C for indicated intervals of time. The caspase-3, -8, and -9 activities were analyzed. The values represent the mean ± SD of three independent experiments. *p < 0.05, differs between I3C treatment and control. For Western blotting analysis, cells were treated with I3C for 6, 12, and 18 h. Total protein extracts were analyzed by immunoblotting with antibodies specific to FADD, Fas, cytochrome c, GADD153, GRP78, and caspase-12. After WEHI-3 cells were exposed to I3C, the location of cytochrome c was determined by using a confocal laser microscope as described in Materials and Methods. The representative data are presented from three separate experiments with similar expression.

caspase-3 activities with a colorimetric enzymatic assay. As shown in Figure 5A, only caspase-8 activity increased at 3 h after I3C treatment. The levels of caspase-8, -9, and -3 activities increased at 6, 12, and 18 h after I3C treatment. Our results suggest that I3C-induced apoptosis is mediated through the activation of caspase-8, caspase-9, and then caspase-3.

I3C Affected Apoptotic-Associated Protein Levels and Enhanced Cytochrome c Release from Mitochondria in WEHI-3 Cells. To determine the mechanisms of I3C-induced apoptosis, we investigated the protein expression of FADD, Fas/CD95, GADD153, GRP78, caspase-12, and cytochome c with Western blotting analysis on I3C-treated WEHI-3 cells. As shown in Figure 5B, the protein levels of FADD, GRP78, GADD153, capsase-12, and cytochrome c were strongly up-regulated in response to I3C treatment. I3C stimulated cytochrome c release from mitochondria trafficking to cytosol (Figure 5C). Our results suggest that the I3C-induced apoptotic response is mediated by ER stress, FADD-mediated caspase-8, and mitochondria-dependent multiple signaling pathways.

I3C Enhanced Release of Cytochrome c from Mitochondria in WEHI-3 Cells. I3C stimulated cytochrome c release from mitochondria trafficking to cytosol (Figure 5C). The possible signaling pathway for I3C-induced apoptosis can be summarized as shown in Figure 6, indicating that I3C-induced apoptosis also occurs through caspase cascade- and mitochondria-independent signal pathways. Also, I3C triggered G0/G1 phase arrest via regulation of cycln A/E and CDK2 decrease in WEHI-3 cells.

I3C Attenuated the DNA Binding Activity of NF-κB in WEHI-3 Cells. To determine whether the NF-κB pathway was involved in I3C-inducd apoptotic cell death in WEHI-3 cells, the effects of I3C on NF-κB were investigated. Results are shown in Figure 6A, which indicated that I3C inhibited NF-κB activation after the 6 and 12 h treatments in WEHI-3 cells. In addition, results from Western blotting (Figure 6B) showed that the level of NF-κB (p65) from the nuclei fraction was decreased, but there was no significant effect on the NF-κB

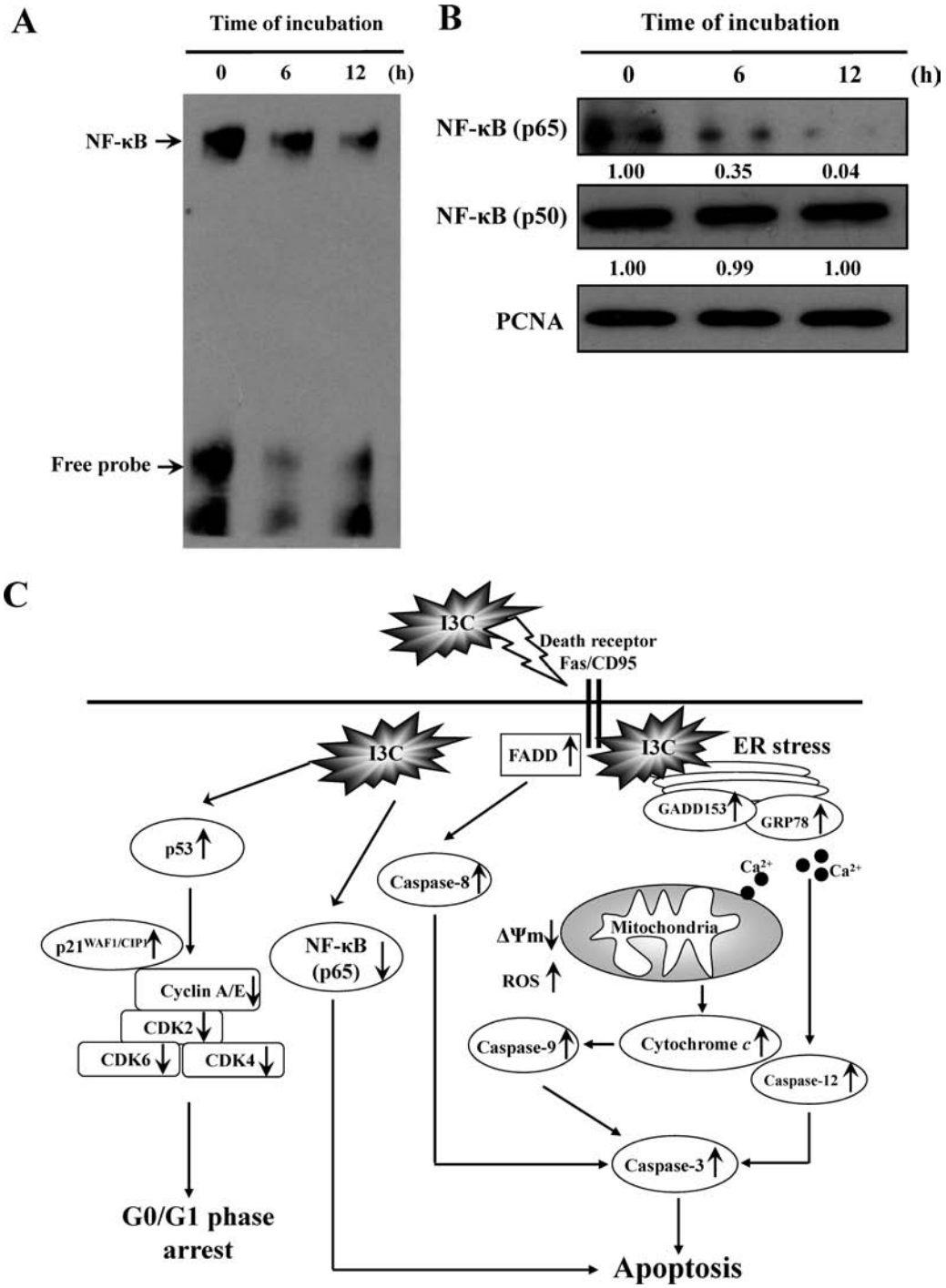

Figure 6. I3C reduced NF-κB DNA binding activity and down-regulated protein expression in WEHI-3 cells. (A) Electrophoretic mobility shift assay (EMSA). Nuclear extracts were prepared from I3C-treated murine leukemia WEHI-3 cells, and NF-κB activity was determined. (B) Effects of I3C treatment in WEHI-3 cells on NF-κB (p65) and NF-κB (p50) protein levels. Each experiment was repeated three times with similar results. (C) Proposed model of the I3C mechanism of action for G0/G1 arrest and apoptosis in WEHI-3 cells. I3C induces p21 expression that led to the decrease of cyclin A, cyclin E, and CDK2 for G0/G1 arrest. Reduction of NF-κB−DNA binding activity and decreased levels of p65 subunit were observed in I3C-treated WEHI-3 cells. I3C induces FADD, GADD153, and GRP78 expression, increases ROS and Ca^{2+} production, and decreases the $\Delta\Psi_m$ level, leading to cytochrome c release and induction of caspase-8, caspase-9, and caspase-3, which then causes apoptosis in WEHI-3 cells.

(p50) protein level in I3C-treated WEHI-3 cells when compared to the 0 h treatment sample.

In Vivo Studies. *I3C Affected the Body, Spleen, and Liver Weights of BALB/c Mice.* After sacrifice, animals from each group were individually weighed and then spleen and liver were isolated and weighed individually. The results shown in Figure 7A−C indicate that I3C increased the body weight (Figure 7A) but significantly decreased the spleen (Figure 7B) and liver (Figure 7C) weights when compared with the untreated leukemia mice.

I3C Affected Cell Markers of White Blood Cells from BALB/c Mice. The whole blood was collected from each mouse of each group, and the cell markers CD3, CD19, CD11b, and Mac-3 were analyzed by flow cytometry. The changes in cell markers of white blood cells from each group are shown in

dx.doi.org/10.1021/jf300963t | J. Agric. Food Chem. 2012, 60, 7634−7643

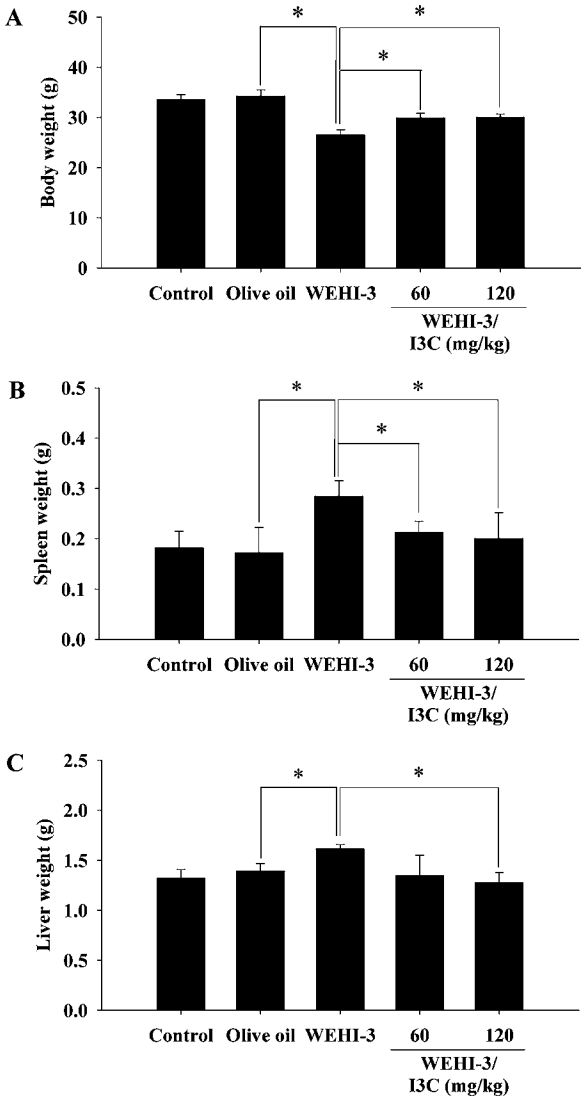

Figure 7. I3C affected the weight of body, spleen, and liver in BALB/c mice. Animals from each group were individually weighed (A) and then individual spleen (B) and liver (C) were isolated and weighed as described in Material and Methods. Each point is mean ± SD (n = 10). *p < 0.05, differs significantly when compared with WEHI-3 cells from the intraperitoneal injection (WEHI-3) group.

Figure 8A–D. These results indicated that I3C increased the levels of CD3 (Figure 8A), reduced the Mac-3 levels (Figure 8D), but did not affect CD19 (Figure 8B) and CD11b (Figure 8D) when compared with the untreated leukemia group.

I3C Promoted Phagocytosis by Macrophages from the PBMC and Peritoneal Cavity of BALB/c Mice. Cells were collected from each animal and were analyzed for phagocytosis by macrophages. Figure 9 shows that I3C at 60 mg/kg promoted and stimulated phagocytotic activity by macrophages. However, it does not show significant effects at the higher dose of I3C (120 mg/kg).

DISCUSSION

Clinical cancer therapies include surgery, radiation, and chemotherapy but have limited effect at the late metastatic stage. Much evidence from pathological studies suggests that cancers could be prevented or their progression slowed.[31] Investigations of the dietary bioactive components that regulate cancer cell survival could play an important role in the development of new agents with low toxicity to prevent and treat cancer. This study was performed to examine how I3C induces apoptosis in leukemia cells. Apoptosis is a potential target for cancer prevention/treatment at various stages of carcinogenesis. The previous studies showed that I3C inhibits growth of breast, prostate, colon, and cervical cancer cells.[14−16,32,33] Our data showed that I3C inhibited the growth of WEHI-3 leukemia cancer cells. The inhibition of cell viability was found to be concentration- and time-dependent. I3C at 100 μM significantly inhibited WEHI-3 cell growth (Figure 1A). This growth inhibition could be due to cell-cycle arrest and apoptosis (Figure 1).

We further found that the I3C-triggered apoptosis in WEHI-3 cells was mediated through extrinsic signaling. Our results indicated that I3C increased Fas/CD95 and FADD levels, leading to activation of caspase-8, which contributes to activation of caspase-3 (Figure 5). When cell apoptosis is induced extrinsically to stress, it involved the binding of extracellular death ligands (Fas ligand) to cognate cell-surface receptors (Fas/CD95), which triggers the recruitment of intracellular adaptor proteins (FADD) for activating the initiator caspase-8.[3]

In the mitochondria-dependent pathway, the cytochrome c released from mitochondria by apoptotic stimulation associates with pro-caspase-9/Apaf-1 to form an apoptosome before triggering caspase-3 activation and eventually leads to apoptosis.[4,5] Bid, a pro-apoptotic Bcl-2 family member, is a specific substrate of caspase-8 in the death-receptor apoptotic signaling pathway. The full-length Bid is localized in cytosol as an inactive precursor. Caspase-8 cleaves Bid, and the t-Bid translocates into the mitochondria and transduces apoptotic signals from the cytoplasm to the mitochondria.[34] We found that I3C increased the level of t-Bid (data not shown), decreased $\Delta\Psi_m$, increased ROS (Figure 4A,B), and then released cytochrome c (Figure 5C) and contributed to the activation of caspase-9. Our results suggest that both the extrinsic and intrinsic pathways are involved in the I3C-mediated regulation of caspase-3 activation in leukemia cells. The previous studies showed that mitochondria and the death receptor play a central role in apoptotic cell death.[3] However, recent studies suggest that apoptosis can be induced by an ER stress pathway.[4,5] Herein, we delineated an ER stress-induced caspase cascade in WEHI-3 cells that is mediated by caspase-12, up-regulating GADD153, GRP78 (Figure 5B), and intracellular Ca^{2+} (Figure 4C). I3C could activate the endoplasmic reticulum (ER) stress apoptotic pathway. In pancreatic cancer cells, I3C analogue 3,3′-diindolylmethane (DIM) has been shown to induce apoptosis through ER-dependent up-regulation of death receptor 5.[35]

By flow cytometry analysis, we found that I3C induced G1 cell-cycle arrest in WEHI-3 cells (Figure 1C), in accord with the report showing that I3C induces G1 cell-cycle arrest in breast and prostate cancer cells.[16,33] We examined the status of cyclins, cyclin-dependent kinases (CDK), and CDK inhibitors (CDKI) in I3C-treated WEHI-3 cells. By Western blotting analysis, we found that I3C down-regulated the expression of cyclin A and CDK2 and up-regulated the expression of $p21^{WAF1}$ in a concentration-dependent manner (Figure 2). These findings were consistent with results showing cell-growth inhibition and cell-cycle arrest induced by I3C, suggesting that I3C inhibits the growth of leukemia cells through regulation of genes related to the control of cell proliferation and the cell cycle. Rahman et al. reported that I3C inhibited the cell growth of breast cancer cells (MDA-MB-435) and prostate cancer cells (PC-3) with cell-cycle

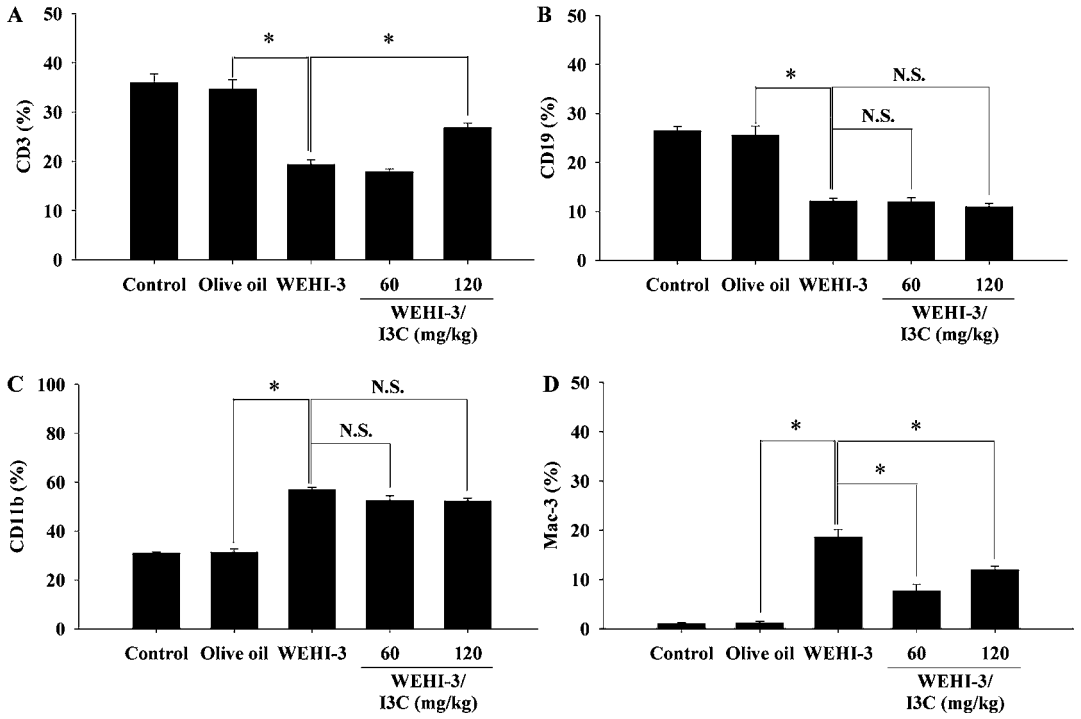

Figure 8. I3C affected cell markers of white blood cells from BALB/c mice. Mice were intraperitoneally injected with WEHI-3 cells (1×10^5 cells/100 μL) for 2 weeks and orally treated without or with 60 and 120 mg/kg I3C for 2 weeks. Blood was collected from each animal and was analyzed for cell markers such as CD3 (A), CD19 (B), CD11b (C), and Mac-3 (D) by flow cytometry as described in Materials and Methods. Each point is mean ± SD, $*p < 0.05$ ($n = 10$), and it is considered significant as compared with WEHI-3 cells from the intraperitoneal injection (WEHI-3) group. N.S., not significant.

arrest in G1 phase and that I3C induced apoptosis in MDA-MB-435 and PC-3 cells with up-regulation of Bax and $p21^{WAF1}$ and down-regulation of Bcl-2.[15] The reports from other laboratories also showed that I3C inhibited the expression of CDK2 and induced G1 arrest in breast and prostate cancer cells.[33] Our results suggest that up-regulation of $p21^{WAF1}$ and the down-regulation of cyclin A/CDK2 and cyclin E/CDK2 may be one of the molecular mechanisms by which I3C inhibits leukemia cell growth and induces cell-cycle arrest. Furthermore, a previous study demonstrated that I3C reduced NF-κB activation and affected NF-κB-regulated antiapoptotic and metastatic genes in myeloid leukemia primary culture cells.[17] We also agree with their report based on our results and data revealing that I3C decreased NF-κB DNA binding activity and the level of p65 protein (Figure 6A,B). Overall, a possible model of the I3C mechanism of action for G0/G1 arrest and apoptosis in WEHI-3 cells is summarized in Figure 6C.

Much evidence has been presented that examines the effect of agents on mice that had been injected with WEHI-3 cells (a murine monomyelocytic leukemia cell line originally derived from the BALB/c mouse).[25,36] We intraperitoneally injected WEHI-3 cells into BALB/c mice and established leukemia mice for I3C treatment. The results demonstrated that I3C statistically decreased the Mac-3 levels and increased the CD3 (T-cell marker) levels but did not show significant effects on CD11b (monocytic marker) and CD19 (B-cell marker) levels in the whole blood from leukemia mice (Figure 8). Results also showed that I3C inhibited spleen leukemia tumor growth in WEHI-3 leukemia mice in vivo (Figure 7B). One of the major characteristics of leukemia mice is the elevation of peripheral monocytes and granulocytes with immature morphology and apparently enlarged and infiltrated spleens as compared with a normal counterpart.[37] In the present study, we determined the enlarged spleen size of the leukemia mice group (injection with WEHI-3 cells only) and observed that I3C decreased the size of spleens (Figure 7B). There was a significant difference between the control and I3C-treated groups. One of the major characteristics in the promotion of immune responses in animal models in vivo is the increased phagocytosis by macrophages.[19,25] In this study, we found that I3C increased macrophage phagocytosis from the PBMC (Figure 9A) and peritoneal cavity (Figure 9B) samples of WEHI-3 leukemia mice. On the basis of these results, it is suggested that antileukemic effects occurred in the I3C-treated leukemia BALB/c mice and that this action might be mediated through alteration of immune responses in vivo. However, the mechanism of immunomodulation for anti-leukemic activity is unclear in this study, and we will investigate this in the future.

In conclusion, we observed the following results from in vitro and in vivo studies: (1) I3C induced cell cycle G0/G1 phase arrest and apoptosis in WEHI-3 leukemia cells. (2) I3C decreased the levels of cyclin A, cyclin D, and CDK2 and increased the levels of $p21^{WAF1/CIP1}$. (3) I3C induced activity of caspase-3, -8, and -9. (4) I3C induced the release of cytochrome c from mitochondria and increased the levels of FADD, GADD153, and GRP78. Our study partly elucidates the molecular mechanisms for using I3C as a potential antitumorigenic agent, and the proposed signal pathways of I3C-tiggered G0/G1 arrest and apoptosis in WEHI-3 cells are shown in Figure 6C. (5) I3C increased the body, spleen, and liver weights in WEHI-3-injected leukemia mice. (6) I3C increased the level of CD3 and decreased the level of Mac-3, but it did not affect the levels of CD11b and CD19. (7) I3C promoted phagocytosis by macrophages in leukemia mice.

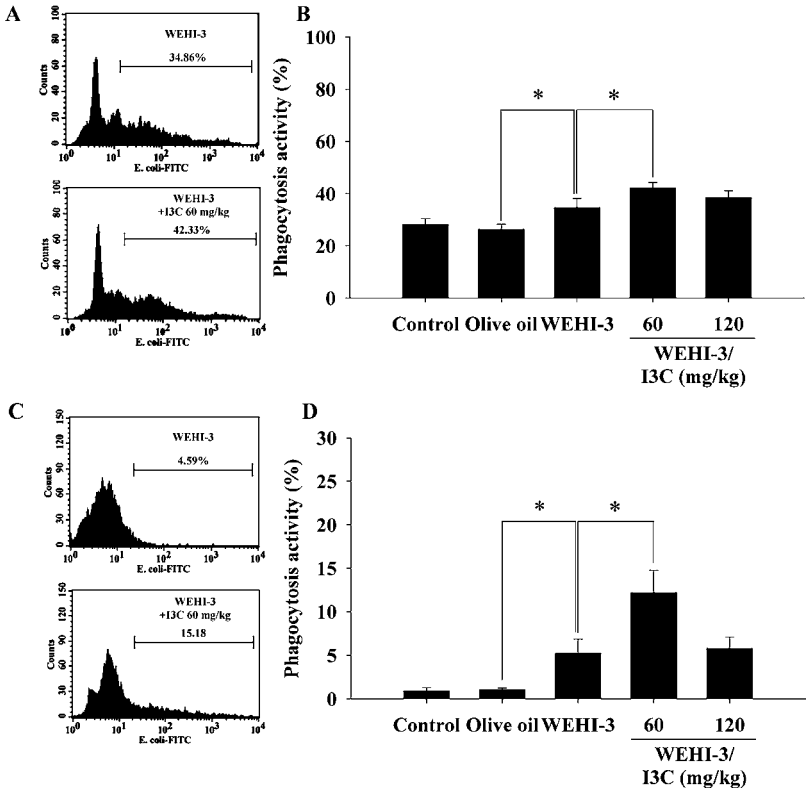

Figure 9. I3C affected phagocytosis by macrophages from BALB/c mice. Mice were intraperitoneally injected with WEHI-3 cells (1×10^5 cells/100 μL) in PBS. After 2 weeks, the mice were orally treated with or without 60 and 120 mg/kg I3C, and then after an additional 2 weeks, macrophages from the PBMC (A) and peritoneal cavity (C) were collected from each animal and analyzed for phagocytotic activity with flow cytometry as described in Materials and Methods. The quantitative results from the flow cytometric data are shown in B and D, respectively, using BD CellQuest software. Each point is mean ± SD. *$p < 0.05$ ($n = 10$), differs significantly when compared with WEHI-3 cells from the intraperitoneal injection (WEHI-3) group.

AUTHOR INFORMATION

Corresponding Author

*(J.-G.C.) Tel.: +886 4 22053366 ext 2161. Fax: +886 4 22053764. E-mail: jgchung@mail.cmu.edu.tw. (Y.-L.C.) Tel.: +886 3 5381183 ext 8174. Fax: +886 3 6102327. E-mail: yunliang@mail.ypu.edu.tw.

Funding Sources

This work was supported by the grant CMU100-ASIA-4 from China Medical University and by the Taiwan Department of Health, China Medical University Hospital Cancer Research Center of Excellence (DOH101-TD-C-111-005).

Notes

The authors declare no competing financial interest.

ABBREVIATIONS USED

AML, acute myelogenous leukemia; Apaf-1, apoptosis protease-activating factor-1; CDK, cyclin-dependent kinase; CDKI, CDK inhibitor; DAPI, 4′,6,-diamidino-2-phenylindole; $DiOC_6$, 3,3′-dihexyloxacarbocyanine iodide; ER, endoplasmic reticulum; H_2DCFDA, 2′,7′-dichlorofluorescin diacetate; I3C, indole-3-carbinol; MTT, 3-(4,5-dimethylthiazol-2-yl)-2,5-diphenyltetrazolium bromide; NAC, *N*-acetylcysteine; ROS, reactive oxygen species; PI, propidium iodide

REFERENCES

(1) Michnovicz, J. J.; Bradlow, H. L. Induction of estradiol metabolism by dietary indole-3-carbinol in humans. *J. Natl. Cancer Inst.* **1990**, *82* (11), 947−949.

(2) Hengartner, M. O. The biochemistry of apoptosis. *Nature* **2000**, *407* (6805), 770−776.

(3) Danial, N. N.; Korsmeyer, S. J. Cell death: critical control points. *Cell* **2004**, *116* (2), 205−219.

(4) Nakagawa, T.; Zhu, H.; Morishima, N.; Li, E.; Xu, J.; Yankner, B. A.; Yuan, J. Caspase-12 mediates endoplasmic-reticulum-specific apoptosis and cytotoxicity by amyloid-beta. *Nature* **2000**, *403* (6765), 98−103.

(5) Scorrano, L.; Oakes, S. A.; Opferman, J. T.; Cheng, E. H.; Sorcinelli, M. D.; Pozzan, T.; Korsmeyer, S. J. BAX and BAK regulation of endoplasmic reticulum Ca^{2+}: a control point for apoptosis. *Science* **2003**, *300* (5616), 135−139.

(6) Sherr, C. J. Cancer cell cycles. *Science* **1996**, *274* (5293), 1672−1677.

(7) Stillman, B. Cell cycle control of DNA replication. *Science* **1996**, *274* (5293), 1659−1664.

(8) el-Deiry, W. S.; Tokino, T.; Velculescu, V. E.; Levy, D. B.; Parsons, R.; Trent, J. M.; Lin, D.; Mercer, W. E.; Kinzler, K. W.; Vogelstein, B. WAF1, a potential mediator of p53 tumor suppression. *Cell* **1993**, *75* (4), 817−825.

(9) Srivastava, B.; Shukla, Y. Antitumour promoting activity of indole-3-carbinol in mouse skin carcinogenesis. *Cancer Lett.* **1998**, *134* (1), 91−95.

(10) Kim, D. J.; Shin, D. H.; Ahn, B.; Kang, J. S.; Nam, K. T.; Park, C. B.; Kim, C. K.; Hong, J. T.; Kim, Y. B.; Yun, Y. W.; Jang, D. D.; Yang, K. H. Chemoprevention of colon cancer by Korean food plant components. *Mutat. Res.* **2003**, *523*−*524*, 99−107.

(11) Rahman, K. W.; Sarkar, F. H. Inhibition of nuclear translocation of nuclear factor-{kappa}B contributes to 3,3′-diindolylmethane-induced apoptosis in breast cancer cells. *Cancer Res.* **2005**, *65* (1), 364−371.

(12) Zhang, J.; Hsu, B. A. J.; Kinseth, B. A. M.; Bjeldanes, L. F.; Firestone, G. L. Indole-3-carbinol induces a G1 cell cycle arrest and inhibits prostate-specific antigen production in human LNCaP prostate carcinoma cells. *Cancer* **2003**, *98* (11), 2511−2520.
(13) Frydoonfar, H. R.; McGrath, D. R.; Spigelman, A. D. Inhibition of proliferation of a colon cancer cell line by indole-3-carbinol. *Colorectal Dis.* **2002**, *4* (3), 205−207.
(14) Kim, D. S.; Jeong, Y. M.; Moon, S. I.; Kim, S. Y.; Kwon, S. B.; Park, E. S.; Youn, S. W.; Park, K. C. Indole-3-carbinol enhances ultraviolet B-induced apoptosis by sensitizing human melanoma cells. *Cell. Mol. Life Sci.* **2006**, *63* (22), 2661−2668.
(15) Rahman, K. M.; Aranha, O.; Glazyrin, A.; Chinni, S. R.; Sarkar, F. H. Translocation of Bax to mitochondria induces apoptotic cell death in indole-3-carbinol (I3C) treated breast cancer cells. *Oncogene* **2000**, *19* (50), 5764−5771.
(16) Moiseeva, E. P.; Heukers, R.; Manson, M. M. EGFR and Src are involved in indole-3-carbinol-induced death and cell cycle arrest of human breast cancer cells. *Carcinogenesis* **2007**, *28* (2), 435−445.
(17) Takada, Y.; Andreeff, M.; Aggarwal, B. B. Indole-3-carbinol suppresses NF-kappaB and IkappaBalpha kinase activation, causing inhibition of expression of NF-kappaB-regulated antiapoptotic and metastatic gene products and enhancement of apoptosis in myeloid and leukemia cells. *Blood* **2005**, *106* (2), 641−649.
(18) Yu, F. S.; Wu, C. C.; Chen, C. T.; Huang, S. P.; Yang, J. S.; Hsu, Y. M.; Wu, P. P.; Ip, S. W.; Lin, J. P.; Lin, J. G.; Chung, J. G. Diallyl sulfide inhibits murine WEHI-3 leukemia cells in BALB/c mice in vitro and in vivo. *Hum. Exp. Toxicol.* **2009**, *28* (12), 785−790.
(19) Tsou, M. F.; Peng, C. T.; Shih, M. C.; Yang, J. S.; Lu, C. C.; Chiang, J. H.; Wu, C. L.; Lin, J. P.; Lo, C.; Fan, M. J.; Chung, J. G. Benzyl isothiocyanate inhibits murine WEHI-3 leukemia cells in vitro and promotes phagocytosis in BALB/c mice in vivo. *Leuk. Res.* **2009**, *33* (11), 1505−1511.
(20) Lu, C. C.; Yang, J. S.; Huang, A. C.; Hsia, T. C.; Chou, S. T.; Kuo, C. L.; Lu, H. F.; Lee, T. H.; Wood, W. G.; Chung, J. G. Chrysophanol induces necrosis through the production of ROS and alteration of ATP levels in J5 human liver cancer cells. *Mol. Nutr. Food Res.* **2010**, *54* (7), 967−976.
(21) Yang, J. S.; Chen, G. W.; Hsia, T. C.; Ho, H. C.; Ho, C. C.; Lin, M. W.; Lin, S. S.; Yeh, R. D.; Ip, S. W.; Lu, H. F.; Chung, J. G. Diallyl disulfide induces apoptosis in human colon cancer cell line (COLO 205) through the induction of reactive oxygen species, endoplasmic reticulum stress, caspases casade and mitochondrial-dependent pathways. *Food Chem. Toxicol.* **2009**, *47* (1), 171−179.
(22) Lu, H. F.; Yang, J. S.; Lai, K. C.; Hsu, S. C.; Hsueh, S. C.; Chen, Y. L.; Chiang, J. H.; Lu, C. C.; Lo, C.; Yang, M. D.; Chung, J. G. Curcumin-induced DNA damage and inhibited DNA repair genes expressions in mouse-rat hybrid retina ganglion cells (N18). *Neurochem. Res.* **2009**, *34* (8), 1491−1497.
(23) Hsia, T. C.; Yang, J. S.; Chen, G. W.; Chiu, T. H.; Lu, H. F.; Yang, M. D.; Yu, F. S.; Liu, K. C.; Lai, K. C.; Lin, C. C.; Chung, J. G. The roles of endoplasmic reticulum stress and Ca^{2+} on rhein-induced apoptosis in A-549 human lung cancer cells. *Anticancer Res.* **2009**, *29* (1), 309−318.
(24) Chen, J. C.; Lu, K. W.; Tsai, M. L.; Hsu, S. C.; Kuo, C. L.; Yang, J. S.; Hsia, T. C.; Yu, C. S.; Chou, S. T.; Kao, M. C.; Chung, J. G.; Wood, W. G. Gypenosides induced G0/G1 arrest via CHk2 and apoptosis through endoplasmic reticulum stress and mitochondria-dependent pathways in human tongue cancer SCC-4 cells. *Oral Oncol.* **2009**, *45* (3), 273−283.
(25) Lu, C. C.; Yang, J. S.; Chiang, J. H.; Hour, M. J.; Lin, K. L.; Lin, J. J.; Huang, W. W.; Tsuzuki, M.; Lee, T. H.; Chung, J. G. Novel Quinazolinone MJ-29 Triggers Endoplasmic Reticulum Stress and Intrinsic Apoptosis in Murine Leukemia WEHI-3 Cells and Inhibits Leukemic Mice. *PloS One* **2012**, *7* (5), e36831.
(26) Chiang, J. H.; Yang, J. S.; Ma, C. Y.; Yang, M. D.; Huang, H. Y.; Hsia, T. C.; Kuo, H. M.; Wu, P. P.; Lee, T. H.; Chung, J. G. Danthron, an anthraquinone derivative, induces DNA damage and caspase cascades-mediated apoptosis in SNU-1 human gastric cancer cells through mitochondrial permeability transition pores and Bax-triggered pathways. *Chem. Res. Toxicol.* **2011**, *24* (1), 20−29.
(27) Wen, Y. F.; Yang, J. S.; Kuo, S. C.; Hwang, C. S.; Chung, J. G.; Wu, H. C.; Huang, W. W.; Jhan, J. H.; Lin, C. M.; Chen, H. J. Investigation of anti-leukemia molecular mechanism of ITR-284, a carboxamide analogue, in leukemia cells and its effects in WEHI-3 leukemia mice. *Biochem. Pharmacol.* **2010**, *79* (3), 389−398.
(28) Lin, M. L.; Chen, S. S.; Lu, Y. C.; Liang, R. Y.; Ho, Y. T.; Yang, C. Y.; Chung, J. G. Rhein induces apoptosis through induction of endoplasmic reticulum stress and Ca^{2+}-dependent mitochondrial death pathway in human nasopharyngeal carcinoma cells. *Anticancer Res.* **2007**, *27* (5A), 3313−3322.
(29) Ahmed, S.; Wang, N.; Hafeez, B. B.; Cheruvu, V. K.; Haqqi, T. M. Punica granatum L. extract inhibits IL-1beta-induced expression of matrix metalloproteinases by inhibiting the activation of MAP kinases and NF-kappaB in human chondrocytes in vitro. *J. Nutr.* **2005**, *135* (9), 2096−2102.
(30) Tan, T. W.; Lin, Y. T.; Yang, J. S.; Lu, C. C.; Chiang, J. H.; Wu, C. L.; Lin, J. P.; Tang, N. Y.; Yeh, C. C.; Fan, M. J.; Chung, J. G. A. cantoniensis inhibits the proliferation of murine leukemia WEHI-3 cells in vivo and promotes immunoresponses in vivo. *In Vivo* **2009**, *23* (4), 561−566.
(31) Weinstein, I. B. Cancer prevention: recent progress and future opportunities. *Cancer Res.* **1991**, *51* (18 Suppl.), 5080s−5085s.
(32) Nachshon-Kedmi, M.; Yannai, S.; Haj, A.; Fares, F. A. Indole-3-carbinol and 3,3′-diindolylmethane induce apoptosis in human prostate cancer cells. *Food Chem. Toxicol.* **2003**, *41* (6), 745−752.
(33) Hsu, J. C.; Dev, A.; Wing, A.; Brew, C. T.; Bjeldanes, L. F.; Firestone, G. L. Indole-3-carbinol mediated cell cycle arrest of LNCaP human prostate cancer cells requires the induced production of activated p53 tumor suppressor protein. *Biochem. Pharmacol.* **2006**, *72* (12), 1714−1723.
(34) Jin, Z.; El-Deiry, W. S. Overview of cell death signaling pathways. *Cancer Biol. Ther.* **2005**, *4* (2), 139−163.
(35) Abdelrahim, M.; Newman, K.; Vanderlaag, K.; Samudio, I.; Safe, S. 3,3′-diindolylmethane (DIM) and its derivatives induce apoptosis in pancreatic cancer cells through endoplasmic reticulum stress-dependent upregulation of DR5. *Carcinogenesis* **2006**, *27* (4), 717−728.
(36) Astashkin, E. I.; Til'kunova, N. A.; Zalepugin, D. Y.; Grachev, S. V. Diallyl sulfide depletes the inositol trisphosphate-sensitive intracellular Ca2+ stores and activates SOC-channels in HL-60 human cells. *Dokl. Biol. Sci.* **2004**, *399*, 500−502.
(37) Warner, N. L.; Moore, M. A.; Metcalf, D. A transplantable myelomonocytic leukemia in BALB-c mice: cytology, karyotype, and muramidase content. *J. Natl. Cancer Inst.* **1969**, *43* (4), 963−982.